Influence of the Dark Exciton State on the Optical and Quantum Optical Properties of Single Quantum Dots

M. Reischle,* G. J. Beirne, R. Roßbach, M. Jetter, and P. Michler

Institut für Halbleiteroptik und Funktionelle Grenzflächen, Universität Stuttgart, Allmandring 3, 70569 Stuttgart, Germany

(Received 28 January 2008; revised manuscript received 18 July 2008; published 1 October 2008)

The dark exciton state strongly affects the optical and quantum optical properties of flat InP/GaInP quantum dots. The exciton intensity drops sharply compared to the biexciton with rising pulsed laser excitation power while the opposite is true with temperature. Also, the decay rate is faster for the exciton than the biexciton and the dark-to-bright state spin flip is enhanced with temperature. Furthermore, long-lived dark state related memory effects are observed in second-order cross-correlation measurements between the exciton and biexciton and have been simulated using a rate-equation model.

DOI: 10.1103/PhysRevLett.101.146402 PACS numbers: 71.35.−y, 78.67.Hc

Quantum dots (QDs) are of high interest to quantum information science. This is because such structures have been shown to be capable of providing single [1], cascaded [2], indistinguishable [3], and entangled photons [4–6] on demand. One complication towards realizing efficient and reliable devices, however, arises from the ubiquitous QD dark exciton state (DS).

In a QD the exciton state (XS) is split as a result of electron-hole (heavy) exchange interaction into a higher energy bright exciton state (BS) and a lower energy dipole forbidden DS with total angular momenta of ± 1 and ± 2, respectively (Fig. 1, inset) [7]. The additional splitting of the BS and DS is comparatively small [7] and is not considered further here. Exciton spin flips may occur via phonon coupling or carrier exchange interactions that can take place on time scales that strongly depend on temperature and dot size and range from roughly 10^{-6} s [8] to 10^{-9} s below 10 K [9]. The biexciton ground state (XX) consisting of spin antipaired electrons and spin antipaired heavy holes does not exhibit such a splitting.

The BS-DS energy difference (ΔE) has been reported to be as low as 10–300 μeV for InGaAs QDs [10,11] and as large as 2–20 meV for colloidal QDs [12,13]. A value of 3.8 meV has been reported for InAs/GaAs QDs [14]. Although the strongly size-dependent splitting for the InP/GaInP QD material system investigated here has been reported to be less than 100 μeV [15], calculations have predicted a value of 5 meV for 3 nm high QDs [16]. The main reason for the very different ΔE values of these dot systems results from the large height differences between them. As ΔE is due to electron-hole exchange interaction, it is proportional to the spatial overlap between the electron and hole. It is thus greatly enhanced for low dimensional structures such as quantum wells [17,18], where values of 2–4 meV, depending on the well thickness, were found, or even more for quantum wires [19]. A further enhancement is observed for QDs as a result of the three-dimensional carrier confinement [13].

Even though ΔE can vary widely, DS effects do influence all QDs. They are simply more apparent when $\Delta E \gg k_B T$, where k_B is Boltzmann's constant and T the temperature. As we have also observed, the DS has been reported to change the ratio of the BS decay time to that of the XX [20]. Even when ΔE is small, under nonresonant pumping, spin uncorrelated electrons and holes should roughly fill the BS and the DS in equal number prior to a spin-flip process. Then if the spin-flip rate is not much faster than the lifetime of the exciton, the DS should exhibit a higher occupation probability than the BS as the DS decays nonradiatively and can consequently be longer lived than the BS. Therefore, nonclassical light sources that make use of the X, such as single-photon sources or entangled-photon sources, will be relatively inefficient and inherently unre-

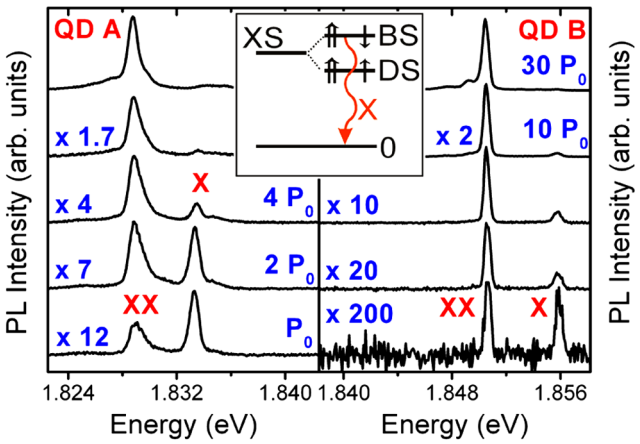

FIG. 1 (color online). PL spectra of QD A and QD B from sample A under pulsed excitation at various PDs ($P_0 = 2$ W/cm^2). XX dominates even at very low PD as a result of the influence of the DS. Inset: Illustration of the splitting of the XS into a BS and a DS which occurs because excitons are composed of electrons ($J_z^e = \pm\frac{1}{2}$) and heavy holes ($J_z^{hh} = \pm\frac{3}{2}$) that can have total angular momenta $J_z^{\mathrm{exc}} = \pm 1$ ($\Uparrow\downarrow$) or $J_z^{\mathrm{exc}} = \pm 2$ ($\Uparrow\Uparrow$).

liable on demand sources. This implies that concepts to avoid DS complications need to be considered for future devices [21]. Furthermore, quantum gates making use of the X should also be adversely affected.

In terms of direct application, the long-lived DS could conceivably be implemented in future storage devices. In addition, dark states have recently been proposed to be usable in quantum information processing [22]. Simon and Poizat [23] have proposed that single-photon emitters such as QDs may, when initially prepared in a metastable state, such as the QD DS, provide a route toward the generation of time-bin-entangled photons [24].

In this Letter, we report the observation of a large ΔE (several meV) in high aspect ratio (width/height $\simeq 27$) InP/GaInP QDs [25] and examine the effect of the DS on the optical and quantum optical properties of QDs.

The samples were grown by metal-organic vapor phase epitaxy on (100) GaAs substrates. The QDs were embedded in GaInP barriers and were grown by depositing two monolayers of InP at 710 °C. In the case of sample A, mesas with diameters of 200 nm were then fabricated in order to enable the investigation of single QDs. Sample B was grown under identical growth conditions with the exception that a distributed Bragg reflector mirror consisting of 45 quarter wavelength pairs of AlAs/AlGaAs was grown underneath the dots in order to enhance the photoluminescence (PL) collection efficiency. In this case a Cr mask with 500 nm diameter apertures was used to isolate individual QDs.

For the micro-PL measurements, the samples were mounted in a He-flow cryostat and were nonresonantly excited using a frequency-doubled Ti:sapphire laser at 410 nm with a repetition rate of 76.2 MHz. The PL was dispersed using a 0.75 m spectrometer and detected using a charge-coupled-device camera when taking spectra or an avalanche photodiode (APD) with a 40 ps time resolution when performing time-resolved PL measurements [25]. In second-order cross-correlation measurements (CCMs) the PL was spectrally selected using two monochromators, one in each arm of a Hanbury Brown–Twiss-type setup, and detected using two APDs.

For clarity, we shall define the terms used to represent the various times discussed in the results section here. τ_{BS}: BS decay time; τ_X: X radiative decay time; τ_{XX}: XX radiative decay time; τ_{fl}: BS-DS spin-flip time; and τ_{bfl}: DS-BS spin-flip time. Including τ_{fl}, τ_{BS} may be described using $\tau_{\mathrm{BS}}^{-1} = \tau_X^{-1} + \tau_{\mathrm{fl}}^{-1}$.

Figure 1 shows the PL recorded from two sample A QDs. Please note that the excitation power density (PD) on the two samples is not directly comparable, as sample A has mesa structures while B has a chromium mask. Under pulsed excitation, far from saturation, XX dominates with respect to X. Normally, however, an X transition should follow each XX, and the XX PL intensity (I_{XX}) should therefore be less than or equal to the X intensity (I_X) [20]. Nevertheless, the extracted PD dependent exponents are in line with the expected values at 0.7 and 1.0 for X (linear) and 1.7 and 1.9 for XX (superlinear) from QD A and QD B, respectively.

These observations may be explained by assuming that the DS lies below the BS by a value $\Delta E \gg k_B T$ (344 μeV at 4 K) [Fig. 4(d)]. Then, following an XX decay, the BS radiative decay probability will be reduced as a spin flip to the DS can occur, with the reduction depending on τ_{fl}. This effect is most evident when ΔE is large as τ_{fl} should be relatively short and τ_{bfl} long.

Furthermore, for QD A and QD C (sample B), when the temperature is raised, I_X effectively increases when normalized to the overall ground state intensity (which decreases; see Fig. 2 inset). This ratio $I_X/(I_X + I_{XX})$ versus temperature was fitted using an Arrhenius model (Fig. 2) and a single activation energy, E_A, equal to 5.0 (1.4) meV, for QD A (QD C), could be extracted.

With increasing temperature, $k_B T$ approaches ΔE implying that τ_{bfl} becomes shorter. The BS occupation probability is thus enhanced and I_X should increase relative to $(I_X + I_{XX})$, as observed. E_A is therefore thought to be due to ΔE. The main reason for the large difference in ΔE between dots most probably results from their different sizes. As the dots studied in this work are very flat (1–3 nm), even the minimum height fluctuation, of one InP monolayer (0.57 nm), can lead to a large difference in their electronic properties [25]. Beyond a particular temperature, τ_{bfl} becomes short enough to make BS radiative decay within a single excitation cycle very probable and thus $I_X/(I_X + I_{XX})$ becomes constant [e.g., beyond 45 K (3.88 meV) for QD C].

The influence of the DS on the BS decay rate [11] has also been examined via time-resolved PL. Although the PL decay curves are not monoexponential, this is not assigned

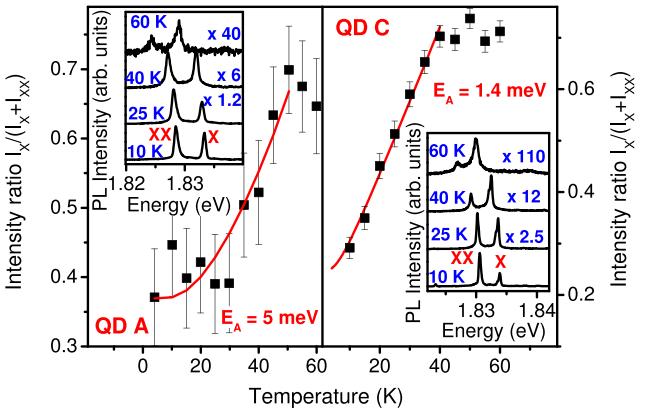

FIG. 2 (color online). Variation of the X intensity relative to the overall ground state intensity (squares) for QD A (PD = 20 W/cm^2) and QD C (PD = 190 W/cm^2). The solid lines are Arrhenius fits obtained using a single activation energy, E_A. The error bars are larger for QD A as a cold-finger cryostat was used. This geometry is less stable than the circular cryostat geometry that was used for QD C. Insets: Spectra from QD A and QD C recorded at different temperatures.

to the DS as this behavior is observed for X and XX. Instead, this is proposed to result from the only partial correlation of electrons and holes in QDs [26]. Therefore we only considered the faster component to estimate the QD PL decay. At 4 K, the average τ_{BS} at 400 ps (dashed gray line) is faster than τ_{XX} which averages 600 ps (solid gray line) (Fig. 3). This is contrary to the simple statistically expected behavior whereby $\tau_{BS} = 2\tau_{XX}$ [20,25,27]. This discrepancy may be explained by the inclusion of DS as an extra decay channel for BS. Assuming that $\tau_X \simeq 2\tau_{XX} = 1200$ ps, we can therefore estimate that $\tau_{fl} \simeq 600$ ps in this case.

As the DS is long-lived, memory effects should be observed in pulsed second-order CCMs, in which the XX emission is the start signal and the X the stop. In such measurements, the time interval between the detection of a photon from transition one by the "start" APD, and the detection of a photon from the other transition by the "stop" APD, is measured using a time-to-amplitude converter. This time interval (coincidence event) is then recorded as one count in one of the channels of a multichannel analyzer. Integrating many such events leads to the buildup of a histogram that displays the temporal correlation between the two transitions [2]. Typically, in a XX-X CCM, one would expect to observe a radiative cascade whereby the probability of detecting X soon after XX is enhanced as manifest by the observation of photon bunching (greater than the Poisson level) for peak 0. This is the expected behavior, as following biexciton decay, an exciton (BS) invariably remains and typically recombines radiatively. This cascade is only clearly observed from QD A [Fig. 4(a)] and is not apparent from QD C [Fig. 4(b)]. However, both QD A and QD C exhibit this cascade in continuous wave CCMs (not presented), thereby excluding the possibility that the low energy peak is due to charged excitonic recombination. Its absence under pulsed conditions for QD C [Fig. 4(b)] may result from the PD being somewhat too high as the observed level of such bunching is known to be strongly PD dependent [28]. For example, for QD A we observed a reduction in the central peak area from 112% to 79%, compared to the Poisson level, when changing the PD from 12 to 30 W/cm^2.

Strong DS related effects have been observed [Figs. 4(a) and 4(b)]. One observes a distinct photon antibunching (less than the Poisson level) of coincidence peak -1 (-13.12 ns delay). This antibunching is strongly PD dependent reaching a minimum value of 42% for QD A at 12 W/cm^2 (63% for QD C at 100 W/cm^2), while for peaks -2 (71%), -3, etc. the respective antibunching becomes successively less pronounced. The antibunching becomes less apparent for both QDs at elevated PDs reaching values of 68% at 30 W/cm^2 (92% at 230 W/cm^2) for peak -1 of QD A (QD C) (not shown). We interpret this behavior as follows. The area of coincidence peak $-n$ represents the probability to detect an XX photon arising from pulse n after a BS photon has been detected from pulse 0. The observed antibunching of peak -1 [Figs. 4(a) and 4(b)] therefore implies that there is a suppressed probability to detect an XX when an X has been detected during the previous pulse cycle. At low PDs, a dot is carrier-free following X decay, and XX detection is therefore improbable during the next cycle (pulse -1). XX emission is, however, more probable for pulse -2 as the DS may have been populated during pulse cycle -1, and

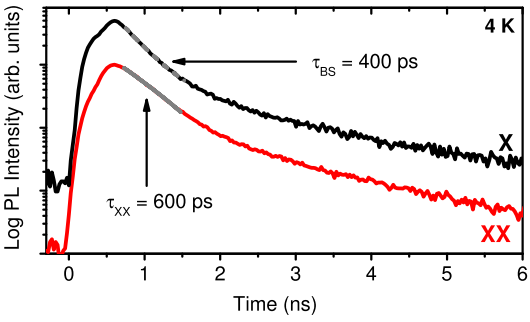

FIG. 3 (color online). Time-resolved PL measurements of the QD C X (BS) and XX at 4 K (PD = 200 W/cm^2). The X trace has been shifted vertically for clarity. The gray lines are exponential fits to the data.

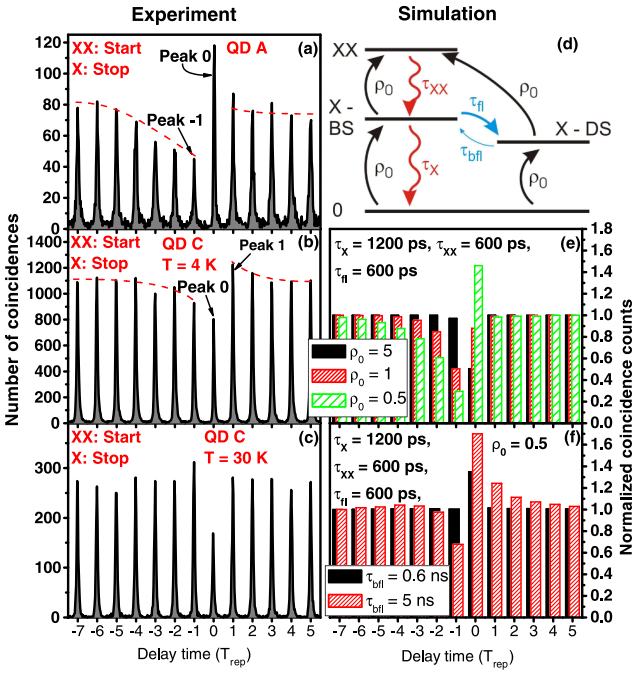

FIG. 4 (color online). (a) CCM between X and XX of QD A (PD = 14 W/cm^2). The distance between the peaks is equal to the time between two laser pulses. (b) CCM between the X and XX of QD C (PD = 150 W/cm^2). The dashed curved lines in (a) and (b) are guides to the eye. (c) As for (b), except that the temperature was raised to 30 K (PD = 150 W/cm^2). (d) Level scheme on which the simulation in (e) and (f) is based (see main text). (e) Simulated XX-X CCM at different powers without considering τ_{bfl}. (f) As for (e) but at a fixed power of 0.5 and including τ_{bfl} (5 ns and 600 ps).

an XX may then be more easily formed via the capture of an electron and hole during pulse cycle -2. In this way the DS effectively stores an X, making XX formation during pulse cycle $n-1$ more probable than during pulse n for $n<0$. This leads to the long-lived memory effects observed in the CCMs. For high peak numbers the two events are successively less correlated and the peak areas approach the Poisson level. Submicrosecond correlations have already been reported from QDs [29,30]; however, the effects were related to charged excitons and the XX-X CCM was symmetric with respect to zero time delay.

The carrier dynamics have been simulated using a rate-equation model that follows the scheme outlined in Fig. 4(d). Besides electron-hole recombination and spin flip, the simulation takes account of QD exciton capture via ρ_0, a dimensionless factor that is proportional to PD. This parameter also connects the short-lived BS (during one cycle), and to a greater extent the long-lived DS (over many cycles), with the XX as the capture of an extra electron-hole pair is sufficient for XX formation when the QD is occupied by either exciton. The results evaluated without including a back spin flip ($\tau_{\mathrm{bfl}}^{-1}=0$) [Fig. 4(e)] simulate the experimental features well [Fig. 4(a)]. Antibunching is only predicted on the negative delay side and is limited to a small number of cycles. In addition, such antibunching disappears at elevated PDs.

Referring to Fig. 4(b), the different ΔE of QD C ($E_A=1.4$ meV) and QD A ($E_A=5$ meV), estimated earlier (Fig. 2), should lead to a different τ_{bfl} for each which in turn influences the CCM behavior. For example, the antibunching of peak -1 for QD C is less pronounced than that of QD A at the lowest PDs. Also, photon bunching of up to 125% is observed for peak 1 of QD C, but not for QD A (104%). Qualitative agreement with experiment can be obtained by adding $\tau_{\mathrm{bfl}}=5$ ns to the model [Fig. 4(f), gray (red) pillars]. One then obtains an antibunching of 87% compared to 30% for the same carrier capture probability without the spin flip [Fig. 4(e), light gray (green) pillars]. Additionally, bunching is predicted for peak 1. At 30 K, DS effects are no longer clearly observed [Fig. 4(c)], probably as a result of a strong decrease in τ_{bfl} with temperature. This effect can be simulated by lowering τ_{bfl} to 600 ps [Fig. 4(f), black pillars]. The correlation behavior then takes on the typical profile with all peaks exhibiting the Poisson normalized level in agreement with experiment, that is except peak 0, which decreases.

Therefore, if $\Delta E > k_B T$ the energetically favorable BS-DS spin flip will be relatively probable while the back DS-BS spin flip will not. At the limit of these conditions, and when the QD is occupied by one electron-hole pair, the X quantum yield, η, is given by $\eta = k_{\mathrm{rad}}(k_{\mathrm{rad}}+k_{\mathrm{nonrad}})^{-1} = \tau_X^{-1}(\tau_X^{-1}+\tau_{\mathrm{fl}}^{-1})^{-1}$, assuming that the spin flip is the only nonradiative channel, where k_{rad} and k_{nonrad} are the radiative and nonradiative recombination rates, respectively. This implies that the X intensity would be reduced by a factor of 3 for the values $\tau_{\mathrm{fl}}=600$ ps and $\tau_X=1200$ ps estimated above.

In summary, we have investigated the influence of the DS on the optical and quantum optical properties of single QDs. The DS is found to reduce the PL intensity and decay time of the X. Therefore, future QD devices based on X decay, such as single-photon sources, or on the XX-X cascade, such as entangled-photon sources, must take the DS into account. Furthermore, we have studied the temperature dependence of the back spin flip (DS-BS) process, and have found that the rate of this process accelerates with temperature. The effects of the DS are thereby reduced and ultimately disappear from view. A distinctly lower energy DS is found to strongly influence the XX-X pulsed second-order cross-correlation function signature. Namely, there is a reduced probability to detect an XX radiative decay following an X detection during the previous pulse cycle. This novel behavior was successfully simulated using a rate-equation model.

Financial support via the DFG Forschergruppe 730 is gratefully acknowledged.

*m.reischle@ihfg.uni-stuttgart.de

[1] P. Michler *et al.*, Science **290**, 2282 (2000).
[2] E. Moreau *et al.*, Phys. Rev. Lett. **87**, 183601 (2001).
[3] C. Santori *et al.*, Nature (London) **419**, 594 (2002).
[4] R. M. Stevenson *et al.*, Nature (London) **439**, 179 (2006).
[5] N. Akopian *et al.*, Phys. Rev. Lett. **96**, 130501 (2006).
[6] R. Hafenbrak *et al.*, New J. Phys. **9**, 315 (2007).
[7] M. Bayer *et al.*, Phys. Rev. B **65**, 195315 (2002).
[8] E. Tsitsishvili, R. V. Baltz, and H. Kalt, Phys. Rev. B **67**, 205330 (2003).
[9] E. Tsitsishvili, R. V. Baltz, and H. Kalt, Phys. Rev. B **72**, 155333 (2005).
[10] M. Bayer *et al.*, Phys. Rev. B **61**, 7273 (2000).
[11] G. A. Narvaez *et al.*, Phys. Rev. B **74**, 205422 (2006).
[12] M. Furis *et al.*, Phys. Rev. B **73**, 241313 (2006).
[13] M. Nirmal *et al.*, Phys. Rev. Lett. **75**, 3728 (1995).
[14] L. Landin *et al.*, Phys. Rev. B **60**, 16640 (1999).
[15] D. W. Snoke *et al.*, Phys. Rev. B **70**, 115329 (2004).
[16] J. Persson *et al.*, Phys. Rev. B **67**, 035320 (2003).
[17] M. Potemski *et al.*, Surf. Sci. **229**, 151 (1990).
[18] Y. Chen *et al.*, Phys. Rev. B **37**, 6429 (1988).
[19] Y. Chen, Phys. Rev. B **41**, 10 604 (1990).
[20] G. Bacher *et al.*, Phys. Rev. Lett. **83**, 4417 (1999).
[21] S. Strauf *et al.*, Nat. Photon. **1**, 704 (2007).
[22] S. E. Economou and T. L. Reinecke, Phys. Rev. Lett. **99**, 217401 (2007).
[23] C. Simon and J.-P. Poizat, Phys. Rev. Lett. **94**, 030502 (2005).
[24] J. Brendel *et al.*, Phys. Rev. Lett. **82**, 2594 (1999).
[25] G. J. Beirne *et al.*, Phys. Rev. B **75**, 195302 (2007).
[26] N. Baer *et al.*, Eur. Phys. J. B **50**, 411 (2006).
[27] M. Wimmer, S. V. Nair, and J. Shumway, Phys. Rev. B **73**, 165305 (2006).
[28] T. Kuroda *et al.*, arXiv:0801.2460.
[29] C. Santori *et al.*, Phys. Rev. B **69**, 205324 (2004).
[30] J. Suffczyński *et al.*, Phys. Rev. B **74**, 085319 (2006).